BIOCHEMISTRY
including biophysical chemistry & molecular biology

Article

pubs.acs.org/biochemistry

Mapping General Anesthetic Binding Site(s) in Human $\alpha1\beta3$ γ-Aminobutyric Acid Type A Receptors with [^{3}H]TDBzl-Etomidate, a Photoreactive Etomidate Analogue

David C. Chiara,[†] Zuzana Dostalova,[§] Selwyn S. Jayakar,[†] Xiaojuan Zhou,[§] Keith W. Miller,[§,‡] and Jonathan B. Cohen*[,†]

[†]Department of Neurobiology and [‡]Department of Biological Chemistry and Molecular Pharmacology, Harvard Medical School, Boston, Massachusetts 02115, United States

[§]Department of Anesthesia, Critical Care, and Pain Medicine, Massachusetts General Hospital, Boston, Massachusetts 02114, United States

Supporting Information

ABSTRACT: The γ-aminobutyric acid type A receptor ($GABA_AR$) is a target for general anesthetics of diverse chemical structures, which act as positive allosteric modulators at clinical doses. Previously, in a heterogeneous mixture of $GABA_ARs$ purified from bovine brain, [^{3}H]azietomidate photolabeling of αMet-236 and βMet-286 in the αM1 and βM3 transmembrane helices identified an etomidate binding site in the $GABA_AR$ transmembrane domain at the interface between the β and α subunits [Li, G. D., et.al. (2006) *J. Neurosci. 26*, 11599−11605]. To further define $GABA_AR$ etomidate binding sites, we now use [^{3}H]TDBzl-etomidate, an aryl diazirine with broader amino acid side chain reactivity than azietomidate, to photolabel purified human FLAG-$\alpha1\beta3$ $GABA_ARs$ and more extensively identify photolabeled $GABA_AR$ amino acids. [^{3}H]TDBzl-etomidate photolabeled in an etomidate-inhibitable manner β3Val-290, in the β3M3 transmembrane helix, as well as α1Met-236 in α1M1, a residue photolabeled by [^{3}H]azietomidate, while no photolabeling of amino acids in the αM2 and βM2 helices that also border the etomidate binding site was detected. The location of these photolabeled amino acids in $GABA_AR$ homology models derived from the recently determined structures of prokaryote (GLIC) or invertebrate (GluCl) homologues and the results of computational docking studies predict the orientation of [^{3}H]TDBzl-etomidate bound in that site and the other amino acids contributing to this $GABA_AR$ intersubunit etomidate binding site. Etomidate-inhibitable photolabeling of β3Met-227 in βM1 by [^{3}H]TDBzl-etomidate and [^{3}H]azietomidate also provides evidence of a homologous etomidate binding site at the $\beta3-\beta3$ subunit interface in the $\alpha1\beta3$ $GABA_AR$.

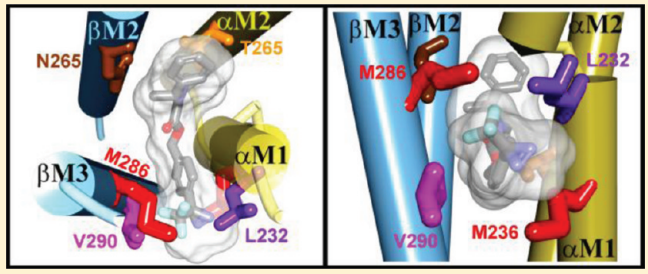

General anesthetics have been employed to relieve surgical suffering for some 165 years, but their sites of action have proven to be hard to define. Inhaled anesthetics act at relatively high concentrations ($\sim10^{-4}$ M), and their pharmacologies are complex and multifactorial. In contrast, some intravenous agents act at sufficiently low concentrations ($\sim10^{-6}$ M) to exhibit relatively specific pharmacology.[1,2] Prime among these is etomidate, an agent that acts in the low micromolar range.[3] (*R*)-Etomidate is 10 times more potent than (*S*)-etomidate in anesthetic potency, a degree of enantioselectivity rare for a general anesthetic, and physiological studies demonstrate the same enantioselectivity for the γ-aminobutyric acid type A receptors ($GABA_ARs$).[4] At low concentrations, etomidate enhances currents elicited by subsaturating concentrations of GABA, whereas at higher concentrations, it can elicit currents in the absence of GABA. These actions are consistent with a model in which the low occupancy of two equivalent etomidate binding sites enhances GABA-elicited currents and high occupancy induces gating independent of the GABA site.[5]

$GABA_ARs$ belong to the Cys loop superfamily of receptors, each consisting of five identical or homologous subunits arranged pseudosymmetrically around a central ion pore.[6,7] The transmembrane domain of each subunit consists of a loose bundle of four α helices (M1−M4), with amino acids on one face of each M2 helix forming the lumen of the ion channel. Etomidate's action depends strongly on the subunit composition of $GABA_ARs$, with the presence of $\beta2$ or $\beta3$ subunits necessary for high sensitivity.[8] On the basis of studies with chimeric β subunits, mice containing a point mutation (N265M) in the M2 helix of the $\beta3$ subunit were created, and etomidate's potency was shown to be strongly attenuated.[9,10]

The latter studies define one molecular target of etomidate's in vivo action, those $GABA_ARs$ that contain $\beta3$ subunits, but they do not determine whether the point mutation modifies the

Received: November 30, 2011
Revised: January 10, 2012
Published: January 13, 2012

etomidate binding site or alters anesthetic potency allosterically. In the absence of high-resolution structures, one strategy for locating the binding site is to develop photoactivatable general anesthetics that are stable under normal conditions but insert covalently into their binding site when activated by UV irradiation. The first such etomidate derivative, azietomidate, mimicked etomidate faithfully.[11] It was equipotent as a general anesthetic and a $GABA_AR$ potentiator, and it exhibited similar enantioselectivity. Furthermore, introduction of the β3N265M point mutation into mice attenuated azietomidate's general anesthetic potency.[12] These studies strongly suggest that etomidate and azietomidate act at the same site.

Employing [^{3}H]azietomidate to photolabel a heterogeneous population of $GABA_ARs$ purified from bovine brain, etomidate-inhibitable photoincorporation was found in two residues, Met-236 (α1 numbering) within an α subunit M1 helix and Met-286 in a β subunit M3 helix.[13] On the basis of a $GABA_AR$ homology model derived from the structure of the *Torpedo* nicotinic acetylcholine receptor (nAChR),[14] it was hypothesized[13] that etomidate bound in the transmembrane domain in a pocket between the β and α subunits of a single $GABA_A$ receptor, the interface between subunits that also contains the GABA binding site in the extracellular domain. Although this was the first direct identification of amino acids contributing directly to a $GABA_AR$ anesthetic binding site, definition of the structure of the etomidate binding site was limited by several factors. (i) The diversity of $GABA_AR$ subunit combinations purified on the benzodiazepine affinity column and the high degree of sequence identity in the regions of primary structure containing the photolabeled amino acids precluded the identification of the photolabeled α and β subunit subtypes. (ii) This $GABA_AR$ heterogeneity, in conjunction with the limited quantities of $GABA_AR$ that can be purified from brain and the fact that photoactivated azietomidate can react only with nucleophilic, but not aliphatic, amino acid side chains,[15,13,16] made difficult the identification of photolabeled amino acids in other regions of primary structure. (iii) The validity of $GABA_AR$ homology models derived from *Torpedo* nAChR structure, the only structure then available, but whose subunits lack sequence and length conservation with $GABA_AR$ subunits in the M3 region, was uncertain. In other such homology models,[17,18] one or both of the photolabeled amino acids were not located at the $\beta-\alpha$ interface.

To circumvent these limitations, in this work we photolabel purified human FLAG-α1/β3 $GABA_ARs$[19] with a novel photoreactive etomidate analogue, [^{3}H]TDBzl-etomidate (Figure 1),

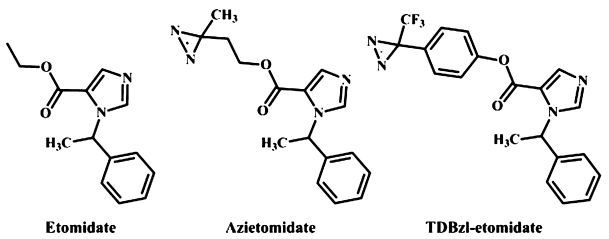

Figure 1. Structures of etomidate and its photoreactive derivatives.

and we interpret the results using $GABA_AR$ homology models based upon the recently determined structures of prokaryote (GLIC[20]) and invertebrate (GluCl[21]) homologues that have a high degree of amino acid sequence conservation with respect to the $GABA_AR$ M3 and M4 helices. TDBzl-etomidate acts as a positive modulator of the $GABA_AR$ at concentrations producing anesthesia,[22] and when photoactivated, it forms a carbene that can react with most amino acid side chains, including aliphatics.[23] This broad side chain reactivity makes [^{3}H]TDBzl-etomidate a favorable probe for determining the extent of the β3–α1 subunit interface contributing to that etomidate binding site and for determining whether etomidate binds to additional sites in the $GABA_AR$. For comparison with photolabeling results obtained with the bovine brain $\alpha\beta\gamma$ $GABA_AR$, we also photolabel the FLAG-α1/β3 $GABA_AR$ with [^{3}H]azietomidate.

EXPERIMENTAL PROCEDURES

Materials. [^{3}H]Muscimol {3-hydroxy-5-aminomethylisoxazole, [*methylene*-^{3}H(N)], 22.5 Ci/mmol} was from Perkin-Elmer (Waltham, MA). *n*-Dodecyl β-D-maltopyranoside, sodium cholate, and 3-[(3-cholamidopropyl)dimethylammonio]-1-propanesulfonate (CHAPS) were from Anatrace-Affymetrix (Anagrade quality). Anti-FLAG M2 affinity gel, FLAG peptide (DYKDDDDK), GABA (γ-aminobutyric acid), polyethylene glycol, γ-globulins from bovine blood, soybean asolectin, and 3-bromo-3-methyl-2-(2-nitrophenylthio)-3*H*-indole (BNPS-skatol, B4651) were from Sigma-Aldrich. [^{3}H]Azietomidate (12 Ci/mmol) and [^{3}H]TDBzl-etomidate (16 Ci/mmol) were synthesized as described previously.[11,22] (*R*)-Etomidate was from Organon Laboratories. *Staphylococcus aureus* glutamic-C endopeptidase (EndoGlu-C) was from Princeton Separations (Adelphia, NJ), and *Lysobacter enzymogenes* lysine-C endopeptidase (EndoLys-C) was from Princeton Separations and Roche Applied Science. Treated trypsin-TPCK was obtained from Worthington Biochemical Corp. *o*-Phthalaldehyde (OPA) was purchased from Alfa Aesar.

Preparation of α1β3 $GABA_A$ Receptors. α1β3 $GABA_ARs$ with a FLAG epitope at the N-terminus of the α1 subunit were expressed in a tetracycline-inducible, stably transfected HEK293S cell line as described previously[19] and purified using a modification of that published procedure. Briefly, membranes from 40–60 plates (15 cm, 1 mg/mL protein; 6–10 nmol of [^{3}H]muscimol binding sites) were solubilized overnight at 4 °C in ~300 mL of purification buffer [50 mM Tris-HCl (pH 7.4), 150 mM NaCl, 2 mM $CaCl_2$, 5 mM KCl, 5 mM $MgCl_2$, 4 mM EDTA, 20% glycerol, pepstatin, chymostatin, and leupeptin (10 μg/mL each), 2 μg/mL aprotinin, and 1 mM phenylmethanesulfonyl fluoride] supplemented with 2.5 mM *n*-dodecyl β-D-maltopyranoside and then centrifuged at 100000*g* for 30 min. Aliquots of supernatant (60–80 mL) were incubated for 2 h at 4 °C with 2 mL of Anti-FLAG M2 affinity resin (capacity of ~2 nmol of [^{3}H]muscimol binding sites) that had been pretreated with poly-D-lysine HBr as described previously,[19] which was then transferred to five Bio-Rad Econo columns. The columns at 4 °C were washed with 6 bed volumes of lipid-exchange buffer (purification buffer supplemented with 17 mM cholate and 8.5 mM asolectin), agitated for 30 min with 5 volumes of lipid-exchange buffer, washed with 2 volumes of lipid-exchange buffer, and then washed with 3 volumes of wash buffer (purification buffer supplemented with 11.5 mM cholate and 0.86 mM asolectin). Receptors were eluted by incubating the resin for 5–10 min with five to six successive batches (0.5 bed volume each) of elution buffer (wash buffer supplemented with 0.1 mM FLAG peptide). The parallel elutions from each of the columns were pooled, aliquoted, frozen, and stored at −80 °C. Aliquots from each pooled elution were characterized by sodium dodecyl sulfate–polyacrylamide gel electrophoresis (SDS–PAGE) for purity and by [^{3}H]muscimol binding for receptor concentration and anesthetic modulation. Individual purifications

dx.doi.org/10.1021/bi201772m | *Biochemistry* 2012, 51, 836–847

started from membranes containing 11−12 nmol of [^{3}H]-muscimol binding sites (2 pmol/mg of protein) and typically resulted in ∼1.5 nmol of purified receptor (50−60 nM binding sites) in 15−25 mL of elution buffer.

Radioligand Binding Assays. Binding of [^{3}H]muscimol to purified $GABA_AR$ was measured by filtration after receptor precipitation with polyethylene glycol.[13] To measure the total number of sites, the sample tube contained 12 nM [^{3}H]-muscimol (final concentration) and 35−70 μL of purified $GABA_AR$, diluted to 3.6 mL in assay buffer [200 mM KCl, 10 mM phosphate buffer (pH 7.4), 1 mM EDTA, and 5 mM CHAPS]. Because of nonspecific binding, a subsaturating concentration of [^{3}H]muscimol was used, and the number of sites was calculated from the dissociation constant (K_D = 10 nM) as described previously.[19] To measure anesthetic modulation, the sample (3.6 mL in assay buffer) contained 350−1050 μL of purified $GABA_AR$, 1 nM [^{3}H]muscimol (final concentration), and anesthetic. At the start of the incubation, half of each sample was used to measure nonspecific binding, which was determined by addition of 1 mM GABA (final concentration). Samples were equilibrated at 4 °C for 45 min in the absence or presence of anesthetics, and then 1.4 mL of polyethylene glycol (final concentration of 15.5%) and γ-globulins (final concentration of 0.1%) were added to precipitate the $GABA_AR$. Fifteen minutes after this addition, three aliquots of 0.9 mL for each condition were filtered on glass fiber filters (Whatman GF/B) that had been pretreated for 1 h in 0.5% (w/v) poly(ethyleneimine). Filters were washed under vacuum with 7 mL of ice-cold assay buffer supplemented with polyethylene glycol (final concentration of 7%), and the retention of ^{3}H on the dried filters was assessed by liquid scintillation counting. For anesthetic titrations, total binding and nonspecific binding were assessed at each anesthetic concentration, with the total and nonspecific control binding (no added anesthetic) determined in quadruplicate. Specific binding (total − nonspecific) was calculated from the means of the triplicate determinations with error propagation using their standard deviations. The potentiation of specific [^{3}H]muscimol binding (P, as a percentage of the control) at anesthetic concentration x was fit to eq 1:

$$P(x) = (P_{max} - 100)/(1 + EC_{50}/x) + 100 \quad (1)$$

where P_{max} is the maximal potentiation and EC_{50} is the anesthetic concentration causing half-maximal potentiation.

Photoaffinity Labeling. Aliquots of purified $GABA_AR$ in elution buffer (∼65 pmol of [^{3}H]muscimol sites/mL) were used for analytical (3−15 pmol/condition) and preparative (115−130 pmol/condition) scale photolabeling. Appropriate amounts of [^{3}H]azietomidate or [^{3}H]TDBzl-etomidate were transferred to glass tubes, and solvent (methanol) was evaporated under an argon stream. Freshly thawed $GABA_AR$ in elution buffer was then added to the tube, and the dried [^{3}H]photoetomidate was resuspended with intermittent gentle vortexing for a minimum of 30 min to a final concentration of 0.5−10 μM. Aliquots were incubated for 30 min with 1 mM GABA (included to prevent potential photolabeling of the GABA binding sites and to stabilize the $GABA_AR$ in a conformation with a high affinity for etomidate and its analogues) with or without 100 μM etomidate. The samples were then placed in individual wells of a 96-well plastic microtiter plate (Falcon catalog no. 353911, analytical photolabeling) or in a plastic 3.5 cm diameter Petri dish (Falcon catalog no. 3001, preparative labeling) and irradiated on ice for 30 min at a distance of 2 cm with a 365 nm lamp (Spectroline model EN-16, Spectronics, Westbury, NY). After irradiation, the samples were mixed with an equal volume of electrophoresis sample buffer [freshly mixed as one part of 2-mercaptoethanol and nine parts of a solution composed of 40% sucrose, 10% SDS, 2% glycerol, 0.0125% bromophenol blue, and 0.3 M Tris (pH 6.8)], incubated for 15 min, and fractionated by SDS−PAGE.

SDS−PAGE. For analytical scale photolabeling, the incorporation of ^{3}H into individual subunits was quantified by liquid scintillation counting of excised gel bands that had been hydrated in 200 μL of deionized water and incubated in gel cocktail [5 mL of freshly mixed 90% Ecoscint A (National Diagnostics) and 10% TS-2 tissue solubilizer (Research Products, Inc.)] for 3 days.

Because the preparative photolabeling of $GABA_AR$ in a detergent resulted in volumes of 4−5 mL of receptor in sample buffer containing as much as ∼1 mCi of ^{3}H, electrophoresis conditions were optimized to handle the large sample volumes and to allow the containment and removal of the unincorporated ^{3}H directly from the gel prior to staining. For this purpose, 1.5 mm thick Laemmli slab gels (8% acrylamide, 0.32% bisacrylamide resolving gel) that were 16 cm long and 14 cm wide were poured, with a 3 cm stacker layer (4% acrylamide, 0.16% bisacrylamide) and wells that were 5 cm deep and 12 cm wide. The samples were electrophoresed overnight at a constant current of 12 mA, and electrophoresis was stopped when the dye front was 4−5 cm from the bottom end of the gel. Prior to staining, the region of the gel below the dye front was excised, safely removing the majority of the unincorporated ^{3}H. Gels were stained with Coomassie Blue stain. Gel bands of interest from preparative labelings were excised and eluted in 12 mL of elution buffer [100 mM NH_4HCO_3, 0.1% SDS, and 2.5 mM dithiothreitol (pH 8.4), 3 days with constant rocking]. Eluates were filtered, concentrated to <400 μL, precipitated with acetone (75% acetone, >4 h, −20 °C), and resuspended in 100 μL of digestion buffer [15 mM Tris, 500 μM EDTA, and 0.1% SDS (pH 8.5)].

Chemical and Enzymatic Fragmentation. Proteases were suspended in water immediately before being used. Samples were digested at 25 °C with 0.5 unit of EndoLys-C (Roche) for 2 weeks or for 2−3 days with 2.5 μg of EndoLys-C (Princeton Separations) or 5 μg of EndoGlu-C. For digestion with trypsin, samples were first diluted 5-fold with 0.5% Genapol C-100 (Calbiochem) in 50 mM NH_4HCO_3 (pH 7.0), and then $^1/_9$ volume containing 10−20 μg of trypsin in 20 mM $CaCl_2$ was added (final $CaCl_2$ concentration of 2 mM). Chemical cleavage at Trp residues of the protein on PVDF filters was achieved using BNPS-skatol as described previously,[24] except that after precipitation of the excess BNPS-skatol, the digestion solution was loaded onto a Prosorb filter for sequencing.

Reverse-Phase HPLC and Sequence Analysis. Digested samples were fractionated by rpHPLC as described previously.[13] HPLC fractions of interest were slowly drop-loaded onto glass fiber filters (Applied Biosystems catalog no. #401111) at 45 °C until all solvent was evaporated. Prior to sequencing, filters were treated with 15 μL of Biobrene Plus (Applied Biosystems catalog no. 400385). Intact subunit samples containing SDS were loaded onto Prosorb PVDF filters (Applied Biosystems catalog no. 402052) following the Prosorb loading directions. Protein sequence analysis was performed on a Procise 492 protein sequencer (Applied Biosystems) set up to analyze two-thirds of the material from each cycle of Edman degradation for amino acid quantification while the other one-third was collected for ^{3}H determination by scintillation counting. PTH-amino acids were quantified from peak heights, and initial

peptide amounts (I_0) and repetitive yields (R) were determined by fitting the background-subtracted picomoles for a sequence to eq 2:

$$I_x = I_0 R^x \quad (2)$$

where I_x is the number of picomoles of the residue detected in cycle x. Values for amino acids Cys, Trp, Ser, and His were excluded from the fits because of known difficulties with their identification or quantification. The specific incorporation (SI, in counts per minute per picomole) at a single residue was determined by eq 3:

$$\mathrm{SI} = 2 \times (\mathrm{cpm}_x - \mathrm{cpm}_{x-1})/I_x \quad (3)$$

where cpm_x was the counts per minute of ^{3}H in cycle x and I_x was calculated from eq 2. In this equation, cpm_{x-1} was used to estimate the background release of ^{3}H.

For some sequences in which a proline residue was encountered prior to the site of labeling, the sequencing filter was treated with OPA (15 μL of a solution consisting of 4 mg of OPA, 2 mL of acetonitrile, and 10 μL of β-mercaptoethanol) at the beginning of the proline-containing cycle to block further sequencing of contaminating peptides that do not contain a proline in that cycle, thereby confirming that any subsequently detected peak of ^{3}H release originated from the proline-containing peptide.[25,26]

Molecular Modeling. On the basis of previous studies of the subunit composition of expressed αβ $GABA_AR$s,[27,28] homology models with a β3α1β3α1β3 subunit ordering were constructed using Discovery Studio (Accelrys, Inc.) from the recently determined crystal structures of two detergent-purified, homopentameric ligand-gated ion channels: GLIC, a proton-gated channel from the prokaryote *Gloeobacter violaceus*, crystallized at pH 4 in the presence of the general anesthetic propofol [Protein Data Bank (PDB) entry 3P50],[20] and GluCl, a glutamate-gated chloride channel from *Caenorhabditis elegans*, crystallized at pH 4.5 in the presence of the allosteric activator ivermectin and glutamate (PDB entry 3RIF).[21] The high degree of amino acid sequence conservation between the $GABA_AR$ subunit M3 and M4 helices and those of GLIC and GluCl, but not with those of the nAChR subunits, allows a more confident alignment of those $GABA_AR$ regions in the homology models based upon the GLIC or GluCl structures than upon the moderate-resolution cryoelectron microscopy structure of the *Torpedo* nAChR in its native membrane environment (PDB entry 2BG9)[14] that we used previously to create a model of the αβγ $GABA_AR$[13] (see Figure S1 of the Supporting Information for the M1−M4 alignments used for our models).

When the transmembrane helices are depicted in helical wheel diagrams (Figure S2 of the Supporting Information), the identities of the amino acids of βM3 and αM1 contributing to the β3−α1 subunit interface are the same in the models based upon GLIC and GluCl, and the locations differ from those in the model based on the nAChR structure only by counterclockwise (looking down the channel) rotations of amino acids in αM1 and in both M2 helices by ∼40° and 20°, respectively, and by a translation of approximately one helical turn down in M3. Thus, in the GLIC and GluCl models, βMet-286 of βM3 is in register with αLeu-232 in αM1, while in the nAChR-derived model, βMet-286 is in register with αIle-228 (Figure S3 of the Supporting Information). All models are generally consistent with experimental studies positioning αMet-236 and βMet-286 at the β−α interface, based upon the formation of intersubunit disulfide cross-links between βM286C or βF289C and cysteines substituted in αM1.[29] As noted,[21] compared to the GLIC structure, there is an increased distance in the GluCl structure between the M3 and M1 helices at that interface where the allosteric activator ivermectin is bound.

CDocker,[30] a CHARMm-based molecular dynamics simulated annealing program, was used to dock drugs into potential binding pockets in the αβ $GABA_AR$ transmembrane domain (β3−α1 or β3−β3 interfaces, the α1 and β3 subunit helix bundles, and the ion channel) in the homology models based upon the structures of GLIC and GluCl. Details about the parameters used for docking are presented in the Supporting Information. The predicted binding site for TDBzl-etomidate at the β3−α1 interface is presented in Figure 8 and in stereo representation in Figures S4 and S5 of the Supporting Information, including a comparison between the GLIC- and GluCl-derived models. Predicted modes of binding at the β3−β3 interface and in the α1 and β3 subunit helix bundles are shown in Figures S6 and S7 of the Supporting Information.

RESULTS

Photoreactive Etomidate Derivatives Potentiate Binding of Agonists to the Purified α1β3 $GABA_AR$. The binding sites for anesthetics in the $GABA_AR$ are coupled energetically to the agonist site, as evidenced by the capacity of anesthetics of diverse structural classes to enhance GABA responses in cells and, for $GABA_AR$ in membrane fractions, to enhance agonist equilibrium binding affinity.[31,32] This energetic coupling between sites is also preserved in the α1β3 $GABA_AR$ in membranes and after affinity purification,[19] as evidenced by the etomidate enhancement of [^{3}H]muscimol binding. We found that (*R*)-azietomidate and TDBzl-etomidate (up to 100 μM) also enhanced [^{3}H]muscimol binding, by ∼100 and ∼140%, respectively (Figure 2). The concentrations for half-maximal

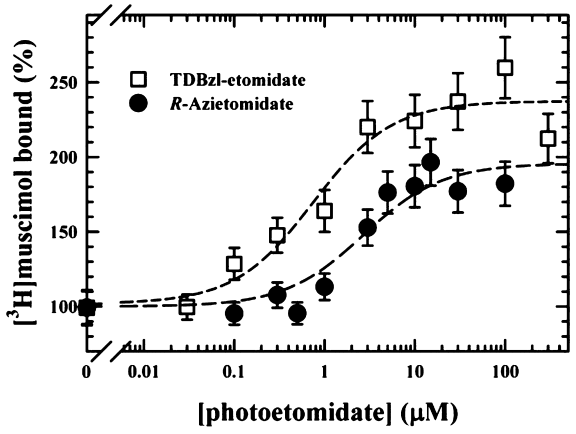

Figure 2. Modulation of binding of [^{3}H]muscimol to the purified α1β3 $GABA_AR$ by photoreactive etomidate derivatives. The purified α1β3 $GABA_AR$ was incubated for 1 h in binding buffer containing 5 mM CHAPS with 1 nM [^{3}H]muscimol, a concentration sufficient to occupy ∼10% of binding sites, and various concentrations of TDBzl-etomidate (□) or (*R*)-azietomidate (●), and then binding was assessed by filtration, as described in Experimental Procedures. Each data point was determined in triplicate and plotted as the mean ± SD. In this typical experiment, the total binding was 4890 ± 21 cpm in the absence of anesthetic, and the nonspecific binding (with 1 mM GABA) was 400 ± 56 cpm. For (*R*)-azietomidate and TDBzl-etomidate, the concentrations producing half-maximal potentiation were 2.7 ± 1.0 and 0.8 ± 0.3 μM, respectively, with maximal potentiations of 200 ± 10 and 240 ± 10%, respectively.

dx.doi.org/10.1021/bi201772m | *Biochemistry* 2012, 51, 836−847

potentiation by (*R*)-azietomidate and TDBzl-etomidate were ~3 and 0.8 μM, respectively. Both values are close to the general anesthetic potencies of these photoreactive anesthetics (EC_{50} = 2.2 and 0.7 μM, respectively[11,22]).

Characterization of the $\alpha1\beta3$ $GABA_AR$. The purity of the $\alpha1\beta3$ $GABA_AR$ was assessed by SDS−PAGE and Coomassie Blue stain, which revealed a major band at ~56 kDa and minor bands at ~59 and ~61 kDa (Figure 3A). When material from each of these bands was extracted and characterized by N-terminal protein sequencing, the primary sequence in both the 59 and 61 kDa bands was the N-terminus of the human $GABA_AR$ $\beta3$ subunit (variant 2, Figure 3B), and the primary sequence in the 56 kDa band was the FLAG-tagged $\alpha1$ subunit (Figure 3C). The $\beta3$ subunit was present in the $\alpha1$ band at ~10% of the level of the $\alpha1$ subunit, and conversely, the $\alpha1$ subunit was present in both $\beta3$ bands at 15−25% of the level of the $\beta3$ subunit.

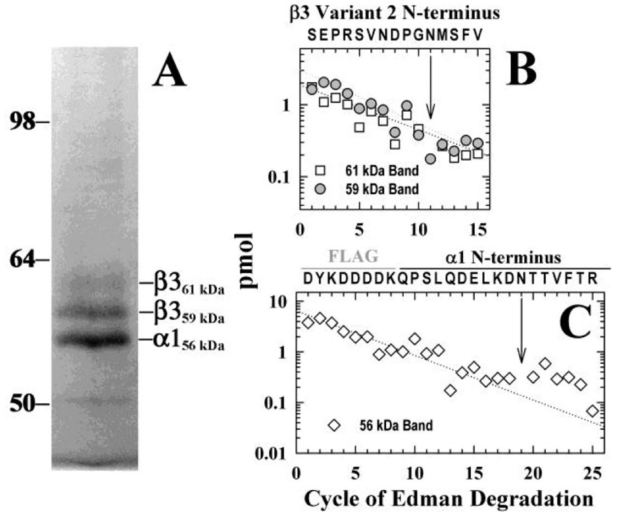

Figure 3. SDS−PAGE and N-terminal sequence analyses of the purified $\alpha1\beta3$ $GABA_AR$. (A) The purity of a $GABA_AR$ preparation was assessed by SDS−PAGE (9 pmol of muscimol binding sites, Coomassie blue stain). (B and C) Picomoles of PTH-amino acids detected during sequencing of material eluted from gel bands of 59 and 61 (B) and 56 kDa (C). The N-terminus of the human $GABA_AR$ $\beta3$ subunit (variant 2) was the primary sequence detected in the 59 and 61 kDa bands (I_0 = 3.0 and 1.9 pmol, respectively), and the FLAG-tagged N-terminus of the $\alpha1$ subunit was the primary sequence in the 56 kDa band (I_0 = 6.5 pmol). The 56 kDa band contained as the secondary sequence 0.6 pmol of $\beta3$, and the 59 and 61 kDa bands each contained 0.4 pmol of FLAG-$\alpha1$. The $\beta3$ subunits in the 59 and 61 kDa bands are differentially glycosylated, as evidenced by the level of PTH-Asn detected in Edman degradation cycle 11 [arrow (see Results)].

The N-terminal sequence analyses also indicated that the $\beta3$ subunits in the 59 and 61 kDa bands differed in terms of their glycosylation at the first consensus N-linked glycosylation site in the subunit. The 11th cycle of Edman degradation of the $\beta3$ subunit and the 19th cycle of the FLAG-$\alpha1$ subunit are predicted to contain asparagines that are potential sites of N-linked glycosylation. No PTH-Asn was released during those cycles of Edman degradation of the 56 kDa $\alpha1$ subunit or the $\beta3$ subunit in the 61 kDa band, consistent with glycosylation at those positions. However, PTH-Asn was released in the 11th cycle for the $\beta3$ subunit in the 59 kDa band, which indicates that the $\beta3$ subunits in the 59 and 61 kDa bands are differentially glycosylated at that position.

Etomidate Inhibits [^{3}H]Azietomidate and [^{3}H]TDBzl-Etomidate Photolabeling of the $\alpha1\beta3$ $GABA_AR$. The $GABA_AR$ in elution buffer was photolabeled, and subunit photolabeling was assessed by SDS−PAGE and liquid scintillation counting of excised gel bands (Figure 4). In the presence of 1 mM GABA, [^{3}H]azietomidate (10 μM) photolabeled both the $\alpha1$ and $\beta3$ subunits, and 100 μM etomidate inhibited by ~85% the labeling of both subunits (Figure 4A). For the $GABA_AR$ photolabeled with 1 μM [^{3}H]TDBzl-etomidate, addition of GABA altered subunit photolabeling by <10% (not shown), and in the presence of GABA, etomidate (100 μM) reduced the level of incorporation of [^{3}H]-TDBzl-etomidate into the $\alpha1$ subunit by 80% and the $\beta3$ subunit by 60% (Figure 4B).

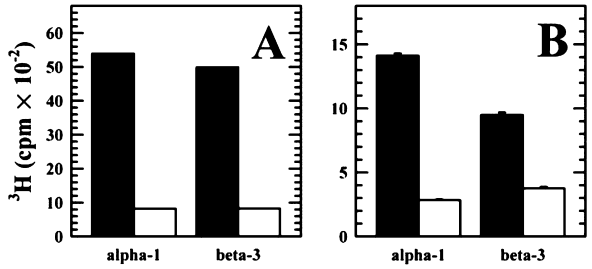

Figure 4. Etomidate-inhibitable photoincorporation of [^{3}H]-azietomidate and [^{3}H]TDBzl-etomidate into $\alpha1\beta3$ $GABA_AR$ subunits. ^{3}H incorporation was assessed by liquid scintillation counting for the gel bands enriched in $\alpha1$ or $\beta3$ subunits isolated by SDS−PAGE from the $\alpha1\beta3$ $GABA_AR$ photolabeled in the presence of 1 mM GABA with 10 μM [^{3}H]azietomidate (A, 16 pmol of muscimol sites) or 1 μM [^{3}H]TDBzl-etomidate (B, 3 pmol of muscimol sites) in the absence (black) or presence (white) of 100 μM etomidate. For the $\beta3$ subunits, the combined counts per minute of ^{3}H in the 59 and 61 kDa gel bands are plotted.

To determine the concentration dependence of [^{3}H]TDBzl-etomidate photolabeling, incorporation of ^{3}H into the $\alpha1$ and $\beta3$ subunits was assessed by SDS−PAGE for the $GABA_AR$ photolabeled by [^{3}H]TDBzl-etomidate at 0.5, 1.5, and 5 μM (total concentrations) in the absence and presence of 100 μM etomidate (Figure 5). In the presence of etomidate, the level of incorporation of ^{3}H into each subunit increased linearly with [^{3}H]TDBzl-etomidate concentration, consistent with a non-specific (or low-affinity) labeling component. The etomidate-inhibitable incorporation into each subunit was fit to a single-site binding model, with a [^{3}H]TDBzl-etomidate concentration of ~0.5 μM associated with half-maximal photolabeling. On the basis of the calculated maximal etomidate-inhibitable photolabeling in the $\alpha1$ subunit (2100 cpm or 0.12 pmol) and $\beta3$ subunit (1420 cpm or 0.08 pmol) and the amount of the $GABA_AR$ (20 pmol of muscimol sites), ~0.6% of $\alpha1$ and 0.4% of $\beta3$ subunits were photolabeled.

[^{3}H]Azietomidate Photolabels $\alpha1$Met-236 and $\beta3$Met-286 in the Human $\alpha1\beta3$ $GABA_AR$. To identify the photolabeled amino acids, the $GABA_AR$ was photolabeled with [^{3}H]azietomidate (700 nM) on a preparative scale (130 pmol of muscimol sites per condition) in the presence of 1 mM GABA in the absence or presence of 100 μM etomidate, and samples containing primarily the $\alpha1$ or $\beta3$ subunit were isolated by SDS−PAGE. The high degree of sequence conservation between bovine and human $GABA_AR$ subunits allowed us to

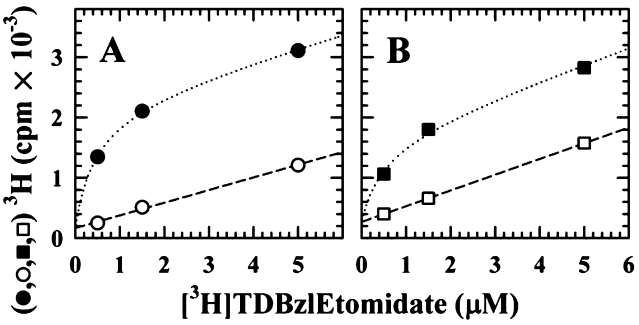

Figure 5. Concentration dependence of [^{3}H]TDBzl-etomidate photolabeling of the $\alpha1\beta3$ $GABA_AR$. Incorporation of ^{3}H into gel bands enriched in $\alpha1$ (A) or $\beta3$ (B) subunits isolated by SDS−-PAGE from the $\alpha1\beta3$ $GABA_AR$ (20 pmol of muscimol sites) photolabeled with [^{3}H]TDBzl-etomidate in the presence of 1 mM GABA and in the absence (● and ■) or presence (○ and □) of 100 μM etomidate. For the samples photolabeled in the presence of etomidate, the counts per minute of subunit increased linearly with [^{3}H]TDBzl-etomidate concentration, with slope B_{ns} and intercept b. For the samples photolabeled in the absence of etomidate, the dotted lines are the fits of the counts per minute of subunit to the equation $f(x) = B_{max}/(1 + K/x) + B_{ns}x + b$, where $f(x)$ is the counts per minute at concentration x, K is the apparent dissociation constant in micromolar, and B_{max} is the maximal etomidate-inhibitable ^{3}H incorporation (in counts per minute). Values of B_{ns} and b were determined from the subunit photolabeling in the presence of 100 μM etomidate. (A) For the $\alpha1$ subunit, $K = 0.45 \pm 0.04$ μM and $B_{max} = 2080 \pm 50$ cpm (120 fmol of ^{3}H) ($B_{ns} = 210 \pm 10$ cpm/μM, and $b = 170 \pm 30$ cpm). (B) For the $\beta3$ subunit, $K = 0.50 \pm 0.18$ μM and $B_{max} = 1420 \pm 130$ cpm (80 fmol of ^{3}H) ($B_{ns} = 260 \pm 10$ cpm/μM, and $b = 270 \pm 10$ cpm).

use the previously developed proteolytic fragmentation and HPLC purification protocols[13] to identify the photolabeled amino acids in the $GABA_AR$ transmembrane domain. HPLC fractions enriched in a $\beta3$ subunit fragment beginning at the C-terminus of the $\beta3$ M2 helix and extending through M3 were isolated from EndoGlu-C digests (Figure S8A of the Supporting Information), and fractions enriched in the $\alpha1$ subunit fragment beginning at the N-terminus of αM1 were isolated from trypsin digests (Figure S9A of the Supporting Information). Those HPLC fractions also contained other subunit fragments, but during sequence analysis, the samples were treated with OPA at the cycles of Edman degradation containing a proline in βM3 (cycle 6, β3Pro-276) or αM1 (cycle 11, α1Pro-233) to prevent further sequencing of contaminating fragments not containing Pro at those cycles.[13,25]

During sequencing of the fragment beginning at β3Thr-271 with OPA treatment at cycle 6 (Figure 6A), the major peak of ^{3}H release was in cycle 16, establishing that β3Met-286 was labeled at 85 cpm/pmol and that the photolabeling was fully inhibited by etomidate. When HPLC fractions containing the fragment beginning at α1Ile-223 were sequenced (Figure 6B) with OPA treatment at cycle 11, the peak of ^{3}H release in cycle 14 established that [^{3}H]azietomidate also photolabeled α1Met-236 in αM1 (130 cpm/pmol) and that the photolabeling could also be fully inhibited by etomidate.[a]

[^{3}H]TDBzl-Etomidate Photolabeling in $GABA_AR$ α1M1 and β3M3. The purified $\alpha1\beta3$ $GABA_AR$ was photolabeled on a preparative scale with [^{3}H]TDBzl-etomidate at two concentrations (2 and 10 μM) in the presence of GABA and in the absence or presence of etomidate (100 μM), and gel band eluates enriched in β3 or α1 subunits were obtained via SDS−PAGE. Photolabeling of amino acids in β3M3 and α1M1 was characterized by sequencing appropriate rpHPLC fractions from EndoGlu-C digests of the β3 subunits (Figure S8B,C of the Supporting Information) and EndoLys-C digests of α1 (Figure S9B,C of the Supporting Information). Representative sequencing data are presented in Figure 6C−F, and amino acid photolabeling efficiencies in the absence and presence of etomidate are summarized in Table 1 in comparison with data for [^{3}H]azietomidate.

For the $GABA_AR$ photolabeled at 2 or 10 μM [^{3}H]TDBzl-etomidate, sequencing of the fractions containing the fragment beginning at β3Thr-271, with treatment with OPA in cycle 6, revealed a major peak of ^{3}H release in cycle 20 (Figure 6C,E), which established that [^{3}H]TDBzl-etomidate photolabeled β3Val-290 and that etomidate inhibited that photolabeling by >90%. For the photolabeling at 10 μM [^{3}H]TDBzl-etomidate (Figure 6E), there were also smaller peaks of ^{3}H release in cycles 16 and 18, which indicated photolabeling of β3Met-286 and β3Cys-288. While etomidate weakened photolabeling of β3Val-290 and β3Met-286 by ≥90 and ∼60%, respectively, photolabeling of β3Cys-288 was enhanced by ∼10% (Table 1).

[^{3}H]TDBzl-etomidate photolabeling of amino acids in αM1 was assessed by sequencing rpHPLC fractions from EndoLys-C digests of α1 subunits that contained the fragment beginning at α1Ile-223 (Figure 6D,F). During sequencing, samples were treated with OPA prior to cycle 11 (α1Pro-233) to prevent further sequencing of contaminating fragments. When material was sequenced from $GABA_AR$ photolabeled at 2 μM [^{3}H]-TDBzl-etomidate (Figure 6D), the peaks of ^{3}H release in cycles 12 and 14 identified photolabeling of α1Cys-234 and α1Met-236, respectively, with etomidate inhibiting photolabeling of those positions by 80 and 60%, respectively. For the photolabeling at 10 μM [^{3}H]TDBzl-etomidate (Figure 6F), the peak of ^{3}H release in cycle 14 indicated photolabeling of α1Met-236, which etomidate reduced by 30%, while photolabeling of α1Cys-234, if it occurred, had an efficiency that was <5% of that of α1Met-236.[b]

[^{3}H]Azietomidate and [^{3}H]TDBzl-Etomidate Also Photolabel β3Met-227 in βM1. Sequence analysis of the rpHPLC fractions containing the major peak of ^{3}H from the EndoGlu-C digest of the [^{3}H]azietomidate photolabeled β3 subunit (Figure S8A of the Supporting Information) identified a β3 subunit fragment beginning at β3Gly-203, 14 amino acids before the beginning of βM1 (Figure 7A). The major peak of ^{3}H release in cycle 25 was consistent with photolabeling of β3Met-227, with etomidate inhibiting that photolabeling by >95%.[a]

Cleavage of the bond between β3Thr-202 and β3Gly-203 was unlikely to be produced by EndoGlu-C, which has specificity for cleavage C-terminal to acidic amino acid side chains. However, [^{3}H]azietomidate photolabeling of β3Met-227 was confirmed by sequence analysis of HPLC fractions from EndoGlu-C digests of [^{3}H]azietomidate photolabeled β subunits from an independent photolabeling experiment (Figure 7B). In this case, a fragment was sequenced beginning at β3His-191, an expected EndoGlu-C cleavage site, and the sample was treated with OPA at cycle 16 (β3Pro-206). The peak of ^{3}H release in cycle 37 confirmed labeling at β3Met-227 in the presence (or absence) of GABA. [^{3}H]TDBzl-etomidate at 10 μM also photolabeled β3Met-227, but with an efficiency that was only ∼20% of that of α1Met-236 (Table 1, data not shown). Thus, β3Met-227 was photolabeled by [^{3}H]azietomidate and [^{3}H]TDBzl-etomidate with the same pharmacological specificity as α1Met-236 in αM1 (Table 1).

dx.doi.org/10.1021/bi201772m | Biochemistry 2012, 51, 836−847

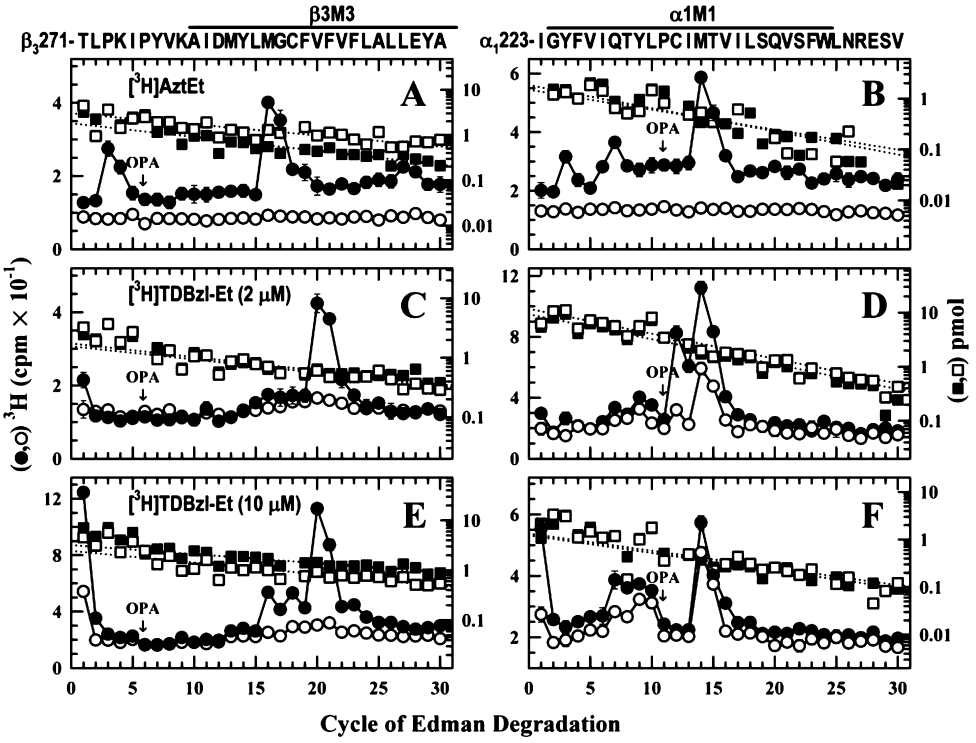

Figure 6. [^{3}H]Azietomidate and [^{3}H]TDBzl-etomidate photolabel amino acids in β3M3 and α1M1. ^{3}H (● and ○) and PTH-amino acids (■ and □) released during N-terminal sequencing of subunit fragments beginning near the N-terminus of βM3 (A, C, and E) or αM1 (B, D, and F) that were isolated by rpHPLC (Figures S1 and S2 of the Supporting Information) from EndoGlu-C digests of β3 subunits and from trypsin (B) or EndoLys-C (D and F) digests of α1 subunits. Aliquots of the α1β3 GABA$_A$R (130 pmol of muscimol sites in 2 mL) were equilibrated with 1 mM GABA and either 700 nM [^{3}H]azietomidate (A and B), 2 μM [^{3}H]TDBzl-etomidate (C and D), or 10 μM [^{3}H]TDBzl-etomidate (E and F) in the absence (● and ■) or presence (○ and □) of 100 μM etomidate (Et) and photolabeled, and then samples containing mostly β3 or α1 subunits were isolated by SDS−PAGE. (A, C, and E) During sequencing of the β3M3 samples, the sequencing filters were treated with OPA prior to cycle 6 (β3Pro-276), thereby ensuring that after cycle 5, only the peptide beginning at β3Thr-271 was sequenced [I_0 without and with Et in picomoles, (A) 1.8 and 3.0, (C) 1.7 and 1.6, and (E) 3.2 and 2.4, respectively]. (A) The peak of ^{3}H release in cycle 16 indicates [^{3}H]azietomidate photolabeling of β3Met-286 (85 cpm/pmol), >95% inhibitable by etomidate. (C and E) The peaks of ^{3}H release in cycle 20 indicate [^{3}H]TDBzl-etomidate photolabeling of β3Val-290 at 83 and 100 cpm/pmol, respectively, with etomidate inhibiting photolabeling by >95%. In panel E, the additional peaks of ^{3}H release in cycles 16 and 18 indicate photolabeling of β3Met-286 (without and with Et, 34 and <6 cpm/pmol, respectively) and β3Cys-288 (without and with Et, 16 and 14 cpm/pmol, respectively). (B, D, and F) Sequence analyses of the α1M1 samples, with OPA treatment prior to cycle 11 (α1Pro-233). After the OPA treatment, only the peptide beginning at α1Ile-223 was sequenced [I_0 without and with Et, in picomoles, (B) 1.8 and 1.5, (D) 7.8 and 10, and (F) 1.2 and 1.3, respectively]. (B) The peak of ^{3}H release in cycle 14 indicates [^{3}H]azietomidate photolabeling of α1Met-236 (130 cpm/pmol), which etomidate inhibited by >95%. (D and F) The peaks of ^{3}H release in cycle 14 indicate [^{3}H]TDBzl-etomidate photolabeling of αMet-236 at 82 and 190 cpm/pmol, respectively, values that were reduced to 32 and 135 cpm/pmol, respectively, in the presence of etomidate. In panel D, the peak of ^{3}H release in cycle 12 indicates photolabeling of α1Cys-234 at 49 and 9 cpm/pmol in the absence and presence of etomidate, respectively.

Does [^{3}H]TDBzl-Etomidate Photolabel Amino Acids in Other Transmembrane Helices? Because TDBzl-etomidate can react with aliphatic as well as nucleophilic amino acid side chains, we also sequenced appropriate HPLC fractions to determine whether it photolabeled amino acids in α1M2, which can be isolated from α1 subunit EndoGlu-C digests, or in α1M4, isolated from EndoLys-C digests. From GABA$_A$Rs photolabeled with [^{3}H]TDBzl-etomidate, sequence analyses of fragments beginning at α1Ser-251 (2 pmol) before α1M2 and of α1Thr-377 (10 pmol) before α1M4 established that any photolabeling of amino acids within α1M2 or α1M4 occurred at a level of <5 cpm/pmol, i.e., at <5% of the photolabeling of α1Met-236 (data not shown).

To evaluate photolabeling in β3M2, an aliquot of intact β3 subunit, isolated from the α1β3 GABA$_A$R photolabeled with 2 μM [^{3}H]TDBzl-etomidate, was digested chemically with BNPS-skatol and sequenced. BNPS-skatol cleaves after Trp residues, of which there are only seven in the β3 subunit. Cleavage at β3Trp-241 near the C-terminus of βM1 allowed sequencing through β3M2 [12 pmol initial yield (Figure S10 of the Supporting Information)]. No release of ^{3}H was detected above background, which indicates that any photolabeling of amino acids in β3M2, if it occurred, was at a level of <5 cpm/pmol, i.e., <10% of the photolabeling of β3Val-290.

■ DISCUSSION

In this report, we identify the amino acids photolabeled in a purified, expressed human FLAG-α1β3 GABA$_A$R by two photoreactive etomidate analogues, [^{3}H]TDBzl-etomidate, which possesses broad amino acid side chain reactivity, and [^{3}H]azietomidate, which can react with nucleophilic but not aliphatic amino acid side chains and was used previously to identify two residues, αMet-236 and βMet-286, photolabeled in a heterogeneous population of the GABA$_A$R purified from bovine brain.[13] We interpret the photolabeling results using α1β3 GABA$_A$R homology models based upon the recently

Table 1. Pharmacological Specificity of Photoincorporation of [^{3}H]Azietomidate and [^{3}H]TDBzl-Etomidate into Residues in the $\alpha1\beta3$ $GABA_AR$ (counts per minute per picomole of PTH derivative)[a]

		[^{3}H]azietomidate		[^{3}H]TDBzl-etomidate			
				2 μM		10 μM	
		without etomidate (cpm/pmol)	with etomidate (% inhibition)	without etomidate (cpm/pmol)	with etomidate (% inhibition)	without etomidate (cpm/pmol)	with etomidate (% inhibition)
αM1							
	α1Cys-234	<5	NQ	55 ± 6	80 ± 2	28 ± 18	<20%
	α1Met-236	165 ± 35	95	90 ± 10	56 ± 4	160 ± 30 (n = 4)	32 ± 8 (n = 3)
βM3							
	β3Met-286	90 ± 5	95	8 ± 4	65 ± 5	32 ± 9 (n = 5)	64 ± 20 (n = 4)
	β3Cys-288	<6	NQ	7 ± 5	−20 ± 30	30 ± 17 (n = 5)	−10 ± 4 (n = 4)
	β3Val-290	<6	NQ	80 ± 10	97 ± 2	90 ± 50 (n = 5)	93 ± 4 (n = 4)
βM1							
	β3Met-227	100 ± 45	>95	ND	ND	43 ± 20	36 ± 6

[a]Incorporation of ^{3}H into each residue was calculated from the observed ^{3}H release and the initial and repetitive yields as described in Experimental Procedures. When more than two samples were sequenced, the number, n, is indicated, and the values are means ± SD. When two samples were sequenced, data are presented as means (±range). The counts per minute per picomole are the values for positions at which the peak of ^{3}H release was >20% over the background release in the previous cycles. The upper limits of the photolabeling in the other cycles were determined from the random variation of the background release of ^{3}H in the adjacent sequencing cycles. For samples photolabeled in the presence of etomidate, the percent inhibition was calculated at each position as the ratio of counts per minute per picomole determined in the presence and absence of etomidate for the paired samples (i.e., same rpHPLC fractions from a digest), and the means (±SD or range) are listed. ND, not determined; NQ, not quantified.

determined crystal structures of two detergent-solubilized, homopentameric ligand-gated ion channels, GLIC, a proton-gated cation-selective channel (PDB entry 3P50),[20] and GluCl, a glutamate-gated chloride channel (PDB entry 3RHW).[21] GLIC and GluCl each have a higher degree of amino acid sequence conservation with the $GABA_AR$ subunit M3 and M4 helices than do the nAChR subunits, and this results in a more confident alignment of those $GABA_AR$ regions in these homology models than in models based upon the structure of the *Torpedo* nAChR (PDB entry 2BG9).[14] As described in Experimental Procedures, the locations of the photolabeled $GABA_AR$ amino acids are essentially equivalent in the homology models based upon these two structures but differ subtly from those in the model we developed previously[13] based upon the *Torpedo* nAChR structure.[c]

Table 1 summarizes, for the purpose of comparison, the efficiencies of photoincorporation of [^{3}H]TDBzl-etomidate and [^{3}H]azietomidate into the $GABA_AR$ amino acids. The locations of the photolabeled amino acids in a $GABA_AR$ homology model based upon the structure of GLIC are shown in Figure 8 in views of the $GABA_AR$ transmembrane domain from the base of the extracellular domain (Figure 8B,D,F) and from the lipid toward the $\beta3-\alpha1$ interface (Figure 8C,E). The photolabeled amino acids β3Met-286, β3Val-290, and α1Met-236 each project into the interface between the $\beta3$ and $\alpha1$ subunits. The photolabeled Cys residues in βM3 (β3Cys-288) and αM1 (α1Cys-234) are not accessible from the pocket at the $\beta3-\alpha1$ interface, despite their proximity in primary structure to β3Met-286/β3Val-290 or α1Met-236. Rather, they project into the $\beta3$ and $\alpha1$ helix bundle pockets, respectively. In a $\beta3\alpha1\beta3\alpha1\beta3$ $GABA_AR$, the photolabeled β3Met-227 in βM1 is located at the interface between adjacent $\beta3$ subunits in the proximity of the photolabeled amino acids in βM3 of the adjacent subunit (Figure 8B,C). In addition to the identification of photolabeled amino acids in αM1, βM1, and βM3, we also established that any [^{3}H]TDBzl-etomidate photolabeling of amino acids in β3M2, α1M2, or α1M4, if it occurred, had an efficiency that was <5% of that of the incorporation in α1Met-236 in α1M1.

Photolabeling and Docking Studies Define a Restricted Etomidate Binding Site at the $\beta3-\alpha1$ Subunit Interface. TDBzl-etomidate, in stick representation, is included in Figure 8D−F docked in a pocket at the $\beta3-\alpha1$ interface in its energy-minimized orientation in the proximity of amino acids from β3M3, β3M2, α1M1, and α1M2, including β3Asn-265 in M2, an etomidate and propofol sensitivity determinant in vitro and in vivo,[9,10] and αLeu-232, a position in αM1 identified as a sensitivity determinant for volatile anesthetics.[1,33] This location is similar to the position in the GluCl structure of ivermectin,[21] a molecule that is much larger than TDBzl-etomidate, which occupies this intersubunit binding site extending between the M3 and M1 helices from the lipid interface to the M2 helices.

In a series of docking calculations testing the effects of different diameter binding site spheres and different initial sets of TDBzl-etomidate conformations and orientations (see Experimental Procedures), in each case for >90 of the 100 lowest-energy docking solutions, (*R*)-TDBzl-etomidate was oriented with its diazirine carbon within 5 Å of the photolabeled residues β3Met-286, β3Val-290, and α1Met-236, and α1Leu-232. The etomidate benzyl group was oriented toward β3Asn-265 and β3Arg-269 (positions M2−15 and M2−19, respectively, in βM2) and α1Gln-229 in αM1 or α1Leu-269 (position M2−14 in αM2) (Figure S4 of the Supporting Information). TDBzl-etomidate is also predicted to be in the proximity of β3Phe-289 and α1Pro-233 (Figure 8F), which are determinants of the shape of this pocket and, therefore, are predicted to be important determinants of the energetics of binding of TDBzl-etomidate. TDBzl-etomidate was also predicted to bind in a similar orientation in this pocket in a $GABA_AR$ homology model based upon the structure of GluCl (Figure S5 of the Supporting Information).

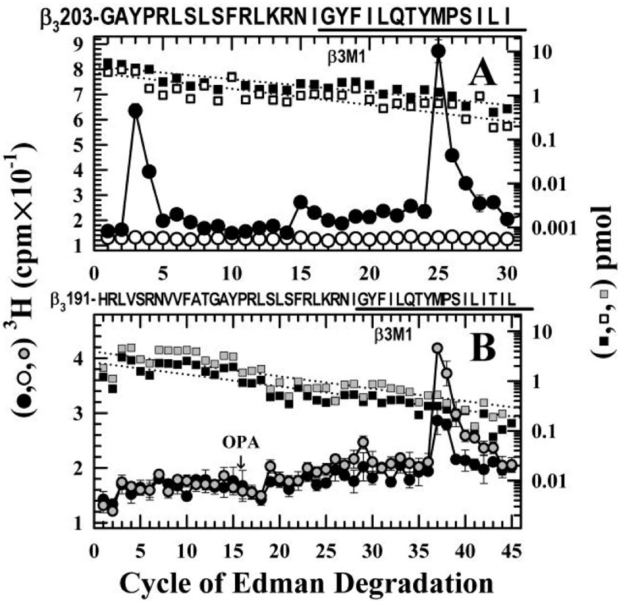

Figure 7. [^{3}H]Azietomidate photolabeling of β3Met-227 in βM1. ^{3}H (● and ○) and PTH-amino acids (■ and □) released during N-terminal sequencing of subunit fragments beginning near the N-terminus of β3M1 that were isolated by rpHPLC (Figure S1A of the Supporting Information) from EndoGlu-C digests of β3 subunits. Aliquots of the $\alpha1\beta3$ GABA$_A$R were photolabeled with 700 nM [^{3}H]azietomidate in the presence of 1 mM GABA in the absence (● and ■) or presence (○ and □) of 100 μM etomidate (Et). (A) The primary sequence began at β3Gly-203 (not an EndoGlu-C cleavage site; I_0 = 1.8 and 1.5 pmol without and with Et, respectively), and the peak of ^{3}H release in cycle 25 indicated photolabeling of β3Met-227 in M1 at 150 cpm/pmol, which etomidate inhibited by >95%.[a] (B) To confirm photolabeling of β3Met-227, a sample was sequenced from EndoGlu-C digests of β3 subunits from another photolabeling in the presence (black symbols) or absence (gray symbols) of GABA. This fragment began at β3His-191 (I_0 = 2.6 and 3.9 pmol with and without GABA, respectively), a predicted EndoGlu-C cleavage site, and the sequencing filters were treated with OPA prior to cycle 16 (β3Pro-207). The peak of ^{3}H release in cycle 37 confirmed [^{3}H]azietomidate photolabeling of β3Met-227 (61 cpm/pmol with GABA and 91 cpm/pmol without GABA).

Because TDBzl-etomidate can react broadly with most amino acid side chains, its photolabeling of β3Val-290, β3Met-286, and α1Met-236, in conjunction with the absence of photolabeling of amino acids in α1M2 and β3M2 and the results of the computational docking studies, provides strong evidence defining the orientation of TDBzl-etomidate in this binding site. Etomidate inhibits photolabeling by 2 μM [^{3}H]TDBzl-etomidate of β3Val-290 by ~90% and photolabeling of β3Met-286 and α1Met-236 by ~60% (Table 1). Although it is not clear why etomidate inhibits [^{3}H]TDBzl-etomidate photolabeling of β3Val-290 more completely, the fact that etomidate inhibits [^{3}H]azietomidate photolabeling of β3Met-286 and α1Met-236 by >90% establishes that etomidate, TDBzl-etomidate, and azietomidate all bind to this site. (*R*)-Etomidate (molecular volume of 205 Å^3) or (*R*)-azietomidate (volume of 240 Å^3) is also predicted to bind within this pocket. However, their predicted orientations within the pocket are less constrained than that of (*R*)-TDBzl-etomidate (volume of 285 Å^3), as a consequence of their smaller sizes.

Photolabeling of β3Met-227 in βM1. [^{3}H]Azietomidate and [^{3}H]TDBzl-etomidate also photolabel β3Met-227, a position in βM1 equivalent to α1Leu-232. [^{3}H]Azietomidate photolabeled β3Met-227 at an efficiency similar to that of α1Met-236 or β3Met-286 (Table 1), and etomidate inhibited [^{3}H]azietomidate photolabeling of β3Met-227 by >95%. In the $\beta3\alpha1\beta3\alpha1\beta3$ GABA$_A$R homology model, β3Met-227 is positioned at a $\beta3-\beta3$ interface and also at the $\alpha1-\beta3$ interface. Docking calculations predict that TDBzl-etomidate can bind in the pocket at the $\beta3-\beta3$ interface, although its orientation may be less constrained than at the $\beta3-\alpha1$ interface (Figure S6 of the Supporting Information). Interestingly, β3Met-227 was not equivalently photolabeled in the $\beta\alpha\beta\alpha\gamma$ GABA$_A$Rs purified from bovine brain,[13] which lack a $\beta-\beta$ interface. The presence or absence of etomidate-inhibitable photolabeling of β3Met-227 in an expressed $\beta3\alpha1\beta3\alpha1\gamma2$ GABA$_A$R will reveal whether etomidate is binding at the unnatural $\beta3-\beta3$ interface in the $\alpha\beta$ GABA$_A$R.

Photolabeling of β3Cys-288 in βM3 and α1Cys-234 in αM1. [^{3}H]TDBzl-etomidate also photolabels β3Cys-288 and α1Cys-234, which in the homology model are located within the pockets in the β3 and α1 subunit helix bundles, respectively (Figure S7 of the Supporting Information). β3Cys-288 and α1Cys-234 of the GABA$_A$R are equivalent to Ile-262 and Met-205 of GLIC, respectively, which in the homopentameric GLIC crystal structure are adjacent in the subunit helix bundle and within 5 Å of the bound propofol.[20]

The photolabeling of β3Cys-288 appears to be consistent with background, nonspecific photolabeling, because aromatic diazirines such as [^{3}H]TDBzl-etomidate are more reactive with Cys than with other amino acid side chains and the observed level of photolabeling increases from 2 to 10 μM but is not inhibited by etomidate (Table 1). However, in the GABA$_A$R homology model, β3Cys-288 is not exposed on the receptor surface but is located deep within the β3 subunit helix bundle pocket. This suggests that TDBzl-etomidate, but not etomidate, can bind with low affinity within this pocket.

α1Cys-234 is located within the α1 subunit helix bundle pocket, and its unusual pharmacology of photolabeling suggests the [^{3}H]TDBzl-etomidate can bind with low affinity within that pocket only when the etomidate or TDBzl-etomidate binding site at the interface between the β3 and α1 subunits is unoccupied. [^{3}H]TDBzl-etomidate at 2 μM photolabeled α1Cys-234 with an efficiency that was ~50% of that of α1Met-236, and etomidate inhibited that photolabeling (Figure 6D and Table 1). However, at 10 μM [^{3}H]TDBzl-etomidate, the level of photolabeling of α1Cys-234 was greatly reduced relative to that of α1Met-236 and insensitive to etomidate (Figure 6F and Table 1). Because [^{3}H]-TDBzl-etomidate at ~1 μM produced ~50% of the maximal etomidate-inhibitable GABA$_A$R photolabeling (Figure 5), these results suggest that α1Cys-234 is not accessible to [^{3}H]TDBzl-etomidate when either etomidate or [^{3}H]TDBzl-etomidate occupies the site at that $\beta3-\alpha1$ interface. α1Cys-234 is accessible to [^{3}H]TDBzl-etomidate when that interfacial site is unoccupied, though TDBzl-etomidate or etomidate may occupy the site at the other $\beta3-\alpha1$ interface.

Diversity of Anesthetic Binding Sites in Pentameric Ligand-Gated Ion Channels. Given the structural diversity of general anesthetics that act as positive GABA$_A$R modulators at clinically relevant concentrations, including small volatiles such as isoflurane and desflurane as well as etomidate, barbiturates, and neurosteroids, it is unlikely that all anesthetics bind to a common class of sites, i.e., at a subunit interface or within a subunit transmembrane helix bundle. Within crystals of GLIC equilibrated with pure propofol or desflurane, which in functional studies act as inhibitors of channel gating, the two anesthetics are bound to

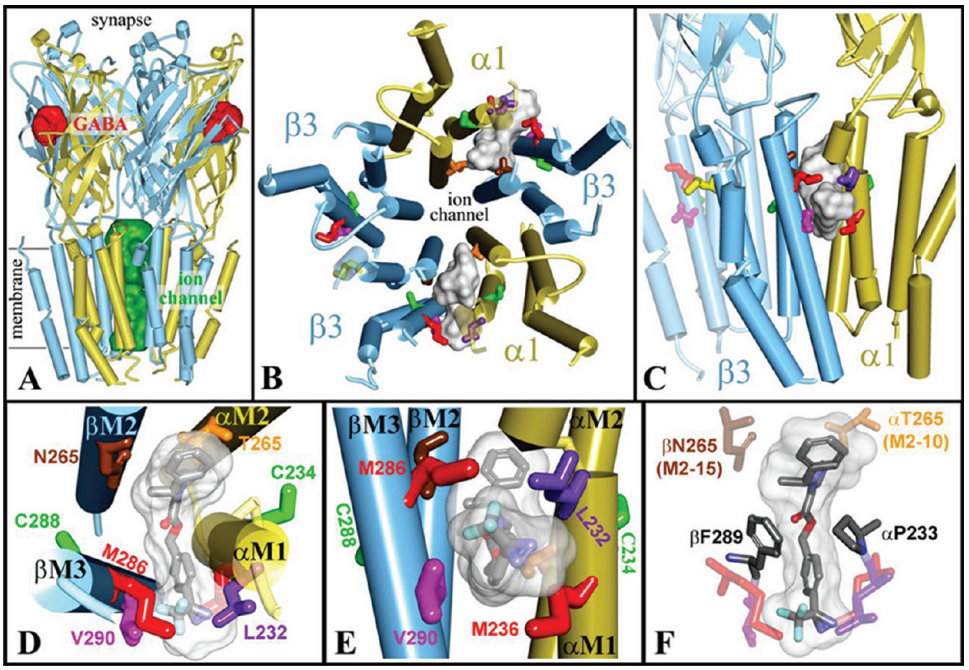

Figure 8. Binding sites for etomidate in the $GABA_AR$ transmembrane domain. (A) Side view of an $(\alpha1)_2(\beta3)_3$ $GABA_AR$ homology model ($\alpha1$, gold; $\beta3$, blue) based upon the structure of GLIC, the *G. violaceus* proton-gated ion channel (PDB entry 3P50).[20] Connolly surface representations are included of the agonist binding sites (red) in the extracellular domain and of the ion channel (green). (B and C) Views of the $GABA_AR$ transmembrane domain from the base of the extracellular domain (B) or from the lipid toward a $\beta3-\alpha1$ interface (C), including Connolly surface representations of the volumes defined by the ensemble of the 100 lowest-energy minimized TDBzl-etomidate docking solutions in the pocket at the $\beta3-\alpha1$ interfaces (volumes of 720 and 820 Å^3). (D and E) Enlargements of the TDBzl-etomidate binding site shown in panels B and C, respectively, with the white transparent Connolly surfaces surrounding the 14 lowest-energy TDBzl-etomidate docking orientations (volume of 510 Å^3). TDBzl-etomidate in its lowest-energy orientation is included in stick format, color-coded with respect to atom type: gray for carbon, red for oxygen, blue for nitrogen, and cyan for fluorine. In panels B–E, the amino acids photolabeled by [^{3}H]TDBzl-etomidate and/or [^{3}H]azietomidate are depicted in stick format with color coding (yellow for $\beta3$Met-227, red for $\beta3$Met-286 and $\alpha1$Met-236, magenta for $\beta3$Val-290, and green for $\alpha1$Cys-234 and $\beta3$Cys-288). Also included in stick format are $\beta3$Asn-265 (βM2–15, brown), an etomidate sensitivity determinant,[9,10] $\alpha1$Leu-232 (in purple), a volatile anesthetic sensitivity determinant,[1,33] and $\alpha1$Thr-265 (M2–10), a position in the *Torpedo* nicotinic acetylcholine receptor α subunit photolabeled by [^{3}H]TDBzl-etomidate.[23] (F) View of the $\beta3-\alpha1$ binding site from the same perspective as panel D, but with the Connolly surface for TDBzl-etomidate in its lowest-energy orientation and including two additional amino acid residues that must have extensive contact with the bound ligand: $\beta3$Phe-289 and $\alpha1$Pro-233. The diazirine carbon is predicted to be within 5 Å of $\beta3$Met-286, $\beta3$Val-290, $\alpha1$Leu-232, and $\alpha1$Met-236; the N atom of $\beta3$Asn-265 and the O atom of $\alpha1$Thr-265 are ~3 Å from the carbon of the CH_3 group and N-3 of the imidazole, respectively.

intrasubunit sites at slightly different depths within the transmembrane helix bundle.[20] In the *Torpedo* nAChR, photoaffinity labeling studies establish that small drugs (volume of <240 Å^3) that act as allosteric inhibitors, including benzophenone, 3-(trifluoromethyl)-3-(*m*-iodophenyl)diazirine, and the general anesthetics halothane and azietomidate, also bind in a state-dependent manner to an intrasubunit site formed by the δ subunit transmembrane helix bundle.[34–38] However, TDBzl-etomidate, which is larger in size (volume of 285 Å^3) and acts as a nAChR potentiator while binding only weakly in the ion channel, binds to a site at the interface between the γ and α subunits.[23] Thus, it remains to be determined whether a drug can act as a $GABA_AR$ potentiator when it binds to an intrasubunit site.

General Anesthetic Binding Sites in $GABA_AR$s. Propofol has been predicted to bind in the proximity of βMet-286, because propofol reduced the kinetics of modification of a cysteine substituted at that position.[39] However, propofol does not bind in a mutually exclusive manner with etomidate, because propofol acts as an allosteric inhibitor of [^{3}H]azietomidate photolabeling of βMet-286 and αMet-236.[40]

The etomidate binding site at the $\beta-\alpha$ interface identified by [^{3}H]azietomidate and [^{3}H]TDBzl-etomidate cannot be a neurosteroid binding site, because neurosteroids enhance, rather than inhibit, $GABA_AR$ photolabeling by [^{3}H]azietomidate.[41] In addition, the single-amino acid substitutions in βM3 and αM1 identified as neurosteroid activation determinants[18] are not located at the $\beta-\alpha$ interface and do not contribute to a common binding site.[7,41]

Volatile anesthetics were proposed to bind to intrasubunit pockets formed by the transmembrane bundle of helices, based upon the locations in an early $GABA_AR$ structural model of anesthetic sensitivity determinants in αM1 (αLeu-232), αM2 (αM2–15), and αM3 (α2Ala-291, equivalent to β3Met-286).[1,33] However, in $GABA_AR$ structural models based upon the structures of the nAChR, GLIC, or GluCl, αLeu-232 and αAla291 are each positioned at interfaces with the β subunit rather than within the helix bundle (Figure 8 and Figures S2–S5 of the Supporting Information; see also ref 42). Further studies using photoreactive analogues of propofol,[43] neurosteroids,[44] or volatile anesthetics[45] will be necessary to determine whether any of these drugs bind in the proximity of the etomidate binding site at the $\beta-\alpha$ interface or, alternatively, to intrasubunit sites within a subunit transmembrane helix bundle or at the protein–lipid interface.

■ ASSOCIATED CONTENT

Supporting Information

Supplemental methods concerning the docking calculations and 10 figures: amino acid sequence alignments used to create the

dx.doi.org/10.1021/bi201772m | *Biochemistry* 2012, 51, 836–847

$GABA_AR$ homology models (Figure S1), helical wheel representations of the transmembrane domain $\beta3-\alpha1$ interface in the 3 $GABA_AR$ homology models (Figure S2), comparison of the $GABA_AR$ transmembrane domain $\beta3-\alpha1$ interfaces in the three $GABA_AR$ homology models (Figure S3), $GABA_AR$ amino acids contributing to the TDBzl-etomidate pocket at the $\beta3-\alpha1$ interface (stereo representation) (Figure S4), stereo-images of TDBzl-etomidate docked into a $\beta3-\alpha1$ interface in homology models derived from the structures of GluCl and GLIC (Figure S5), a pocket at the $GABA_AR$ $\beta3-\beta3$ interface (Figure S6), and the pockets within the $GABA_AR$ α and β subunit helix bundles (Figure S7), rpHPLC fractionations of EndoGlu-C (Figure S8) and trypsin/EndoLys-C (Figure S9) digests of [^{3}H]azietomidate- or [^{3}H]TDBzl-etomidate-photolabeled $GABA_AR$ subunits, and sequence analysis of photoincorporation of [^{3}H]TDBzl-etomidate into $\beta3$M2 (Figure S10). This material is available free of charge via the Internet at http://pubs.acs.org.

AUTHOR INFORMATION

Corresponding Author

*Phone: (617) 432-1728. Fax: (617) 432-1639. E-mail: jonathan_cohen@hms.harvard.edu.

Author Contributions

D.C.C. and Z.D. contributed equally to this work.

Funding

This research was supported by National Institutes of Health Grant GM-58448.

Notes

The authors declare no competing financial interest.

ACKNOWLEDGMENTS

We thank Dr. Ayman Hamouda for many helpful comments about the manuscript.

ABBREVIATIONS

OPA, *o*-phthalaldehyde; GABA, γ-aminobutyric acid; $GABA_AR$, γ-aminobutyric acid type A receptor; nAChR, nicotinic acetylcholine receptor; azietomidate, 2-(3-methyl-3*H*-diaziren-3-yl) ethyl 1-(1-phenylethyl)-1*H*-imidazole-5-carboxylate; TDBzl-etomidate, 4-[3-(trifluoromethyl)-3*H*-diazirin-3-yl]-benzyl 1-(1-phenylethyl)-1*H*-imidazole-5-carboxylate; CHAPS, 3-[(3-cholamidopropyl)dimethylammonio]-1-propanesulfonate; EndoLys-C, *L. enzymogenes* endoproteinase Lys-C; EndoGlu-C, *S. aureus* glutamic-C endopeptidase; rpHPLC, reverse-phase high-performance liquid chromatography; BNPS-skatol, 3-bromo-3-methyl-2-(2-nitrophenylthio)-3*H*-indole; SD, standard deviation.

ADDITIONAL NOTES

[a]In the sequencing data of Figure 6A,B and 7A, the peaks of ^{3}H release in cycle 3 and in cycle 7 (Figure 6B) probably result from [^{3}H]azietomidate photolabeling of $\beta3$Met-227 in βM1 (cycle 3) and $\alpha1$Met-236 in αM1 (cycle 7). We have recently observed that Gln−Thr bonds are susceptible to cleavage under the acidic conditions used to initiate sequencing.[46] This amino acid pair is conserved in M1 of many $GABA_AR$ subunits, with a Thr three residues before $\beta3$Met-227 and seven residues before $\alpha1$Met-236. Direct demonstration of photolabeling of $\beta3$Met-227 by [^{3}H]azietomidate is shown in Figure 7.

[b]The peaks of ^{3}H release in cycles 7 and 9 (Figure 6F) originate from photolabeling in βM3 that contaminates this $\alpha1$ subunit sample.

[c]Comparisons of the locations of the photolabeled amino acids in the GLIC-, GluCl-, and nAChR-derived homology models are shown in Figures S2 and S3 of the Supporting Information.

REFERENCES

(1) Hemmings, H. C., Akabas, M. H., Goldstein, P. A., Trudell, J. R., Orser, B. A., and Harrison, N. L. (2005) Emerging molecular mechanisms of general anesthetic action. *Trends Pharmacol. Sci. 26*, 503−510.

(2) Franks, N. P. (2008) General anaesthesia: From molecular targets to neuronal pathways of sleep and arousal. *Nat. Rev. Neurosci. 9*, 370−386.

(3) Forman, S. A. (2011) Clinical and molecular pharmacology of etomidate. *Anesthesiology 114*, 695−707.

(4) Tomlin, S. L., Jenkins, A., Lieb, W. R., and Franks, N. P. (1998) Stereoselective effects of etomidate optical isomers on γ-aminobutyric acid type A receptors and animals. *Anesthesiology 88*, 708−717.

(5) Rusch, D., Zhong, H. J., and Forman, S. A. (2004) Gating allosterism at a single class of etomidate sites on $\alpha_1\beta_2\gamma_{2L}$ GABA(A) receptors accounts for both direct activation and agonist modulation. *J. Biol. Chem. 279*, 20982−20992.

(6) Cederholm, J. M. E., Schofield, P. R., and Lewis, T. M. (2009) Gating mechanisms in Cys-loop receptors. *Eur. Biophys. J. 39*, 37−49.

(7) Miller, P. S., and Smart, T. G. (2010) Binding, activation and modulation of Cys-loop receptors. *Trends Pharmacol. Sci. 31*, 161−174.

(8) Hill-Venning, C., Belelli, D., Peters, J. A., and Lambert, J. J. (1997) Subunit-dependent interaction of the general anaesthetic etomidate with the γ-aminobutyric acid type A receptor. *Br. J. Pharmacol. 120*, 749−756.

(9) Belelli, D., Lambert, J. J., Peters, J. A., Wafford, K., and Whiting, P. J. (1997) The interaction of the general anesthetic etomidate with the γ-aminobutyric acid type A receptor is influenced by a single amino acid. *Proc. Natl. Acad. Sci. U.S.A. 94*, 11031−11036.

(10) Jurd, R., Arras, M., Lambert, S., Drexler, B., Siegwart, R., Crestani, F., Zaugg, M., Vogt, K. E., Ledermann, B., Antkowiak, B., and Rudolph, U. (2003) General anesthetic actions in vivo strongly attenuated by a point mutation in the GABA(A) receptor $\beta3$ subunit. *FASEB J. 17*, 250−252.

(11) Husain, S. S., Ziebell, M. R., Ruesch, D., Hong, F., Arevalo, E., Kosterlitz, J. A., Olsen, R. W., Forman, S. A., Cohen, J. B., and Miller, K. W. (2003) 2-(3-Methyl-3H-diaziren-3-yl) ethyl 1-(1-phenylethyl)-1H-imidazole-5- carboxylate: A derivative of the stereoselective general anesthetic etomidate for photolabeling ligand-gated ion channels. *J. Med. Chem. 46*, 1257−1265.

(12) Liao, M., Sonner, J. M., Husain, S. S., Miller, K. W., Jurd, R., Rudolph, U., and Eger, E. I. (2005) *R*(+)etomidate and the photoactivable *R*(+)azietomidate have comparable anesthetic activity in wild-type mice and comparably decreased activity in mice with a N265M point mutation in the γ-aminobutyric acid receptor $\beta3$ subunit. *Anesth. Analg. (Hagerstown, MD, U.S.) 101*, 131−135.

(13) Li, G.-D., Chiara, D. C., Sawyer, G. W., Husain, S. S., Olsen, R. W., and Cohen, J. B. (2006) Identification of a $GABA_A$ receptor anesthetic binding site at subunit interfaces by photolabeling with an etomidate analog. *J. Neurosci. 26*, 11599−11605.

(14) Unwin, N. (2005) Refined structure of the nicotinic acetylcholine receptor at 4 Å resolution. *J. Mol. Biol. 346*, 967−989.

(15) Ziebell, M. R., Nirthanan, S., Husain, S. S., Miller, K. W., and Cohen, J. B. (2004) Identification of binding sites in the nicotinic acetylcholine receptor for [^{3}H]azietomidate, a photoactivatable general anesthetic. *J. Biol. Chem. 279*, 17640−17649.

(16) Das, J. (2011) Aliphatic diazirines as photoaffinity probes for proteins: Recent developments. *Chem. Rev. 111*, 4405−4417.

(17) Ernst, M., Bruckner, S., Boresch, S., and Sieghart, W. (2005) Comparative models of GABA(A) receptor extracellular and trans-

membrane domains: Important insights in pharmacology and function. *Mol. Pharmacol. 68*, 1291−1300.
(18) Hosie, A. M., Wilkins, M. E., Da Silva, H. M. A., and Smart, T. G. (2006) Endogenous neurosteroids regulate $GABA_A$ receptors through two discrete transmembrane sites. *Nature 444*, 486−489.
(19) Dostalova, Z., Liu, A. P., Zhou, X. J., Farmer, S. L., Krenzel, E. S., Arevalo, E., Desai, R., Feinberg-Zadek, P. L., Davies, P. A., Yamodo, I. H., Forman, S. A., and Miller, K. W. (2010) High-level expression and purification of Cys-loop ligand-gated ion channels in a tetracycline-inducible stable mammalian cell line: $GABA_A$ and serotonin receptors. *Protein Sci. 19*, 1728−1738.
(20) Nury, H., Van Renterghem, C., Weng, Y., Tran, A., Baaden, M., Dufresne, V., Changeux, J. P., Sonner, J. M., Delarue, M., and Corringer, P. J. (2011) X-ray structures of general anaesthetics bound to a pentameric ligand-gated ion channel. *Nature 469*, 428−431.
(21) Hibbs, R. E., and Gouaux, E. (2011) Principles of activation and permeation in an anion-selective Cys-loop receptor. *Nature 474*, 54−60.
(22) Husain, S. S., Nirthanan, S., Ruesch, D., Solt, K., Cheng, Q., Li, G. D., Arevalo, E., Olsen, R. W., Raines, D. E., Forman, S. A., Cohen, J. B., and Miller, K. W. (2006) Synthesis of trifluoromethylaryl diazirine and benzophenone derivatives of etomidate that are potent general anesthetics and effective photolabels for probing sites on ligand-gated ion channels. *J. Med. Chem. 49*, 4818−4825.
(23) Nirthanan, S., Garcia, G., Chiara, D. C., Husain, S. S., and Cohen, J. B. (2008) Identification of binding sites in the nicotinic acetylcholine receptor for TDBzl-etomidate, a photoreactive positive allosteric effector. *J. Biol. Chem. 283*, 22051−22062.
(24) Crimmins, D. L., McCourt, D. W., Thoma, R. S., Scott, M. G., Macke, K., and Schwartz, B. D. (1990) *In situ* chemical cleavage of proteins immobilized to glass-fiber and polyvinylidenedifluoride membranes: Cleavage at tryptophan residues with 2-(2′-nitrophenylsulfenyl)-3-methyl-3′-bromoindolenine to obtain internal amino acid sequence. *Anal. Biochem. 187*, 27−38.
(25) Brauer, A. W., Oman, C. L., and Margolies, M. N. (1984) Use of *o*-phthalaldehyde to reduce background during automated Edman degradation. *Anal. Biochem. 137*, 134−142.
(26) Middleton, R. E., and Cohen, J. B. (1991) Mapping of the acetylcholine binding site of the nicotinic acetylcholine receptor: [^{3}H]Nicotine as an agonist photoaffinity label. *Biochemistry 30*, 6987−6997.
(27) Tretter, V., Ehya, N., Fuchs, K., and Sieghart, W. (1997) Stoichiometry and assembly of a recombinant $GABA_A$ receptor subtype. *J. Neurosci. 17*, 2728−2737.
(28) Baumann, S. W., Baur, R., and Sigel, E. (2001) Subunit arrangement of γ-aminobutyric acid type A receptors. *J. Biol. Chem. 276*, 36275−36280.
(29) Bali, M., Jansen, M., and Akabas, M. H. (2009) GABA-induced intersubunit conformational movement in the $GABA_A$ receptor α1M1−β2M3 transmembrane subunit interface: Experimental basis for homology modeling of an intravenous anesthetic binding site. *J. Neurosci. 29*, 3083−3092.
(30) Wu, G., Robertson, D. H., Brooks, C. L. I., and Vieth, M. (2003) Detailed analysis of grid-based molecular docking: A case study of CDOCKER—A CHARMm-based MD docking algorithm. *J. Comput. Chem. 24*, 1549−1562.
(31) Sieghart, W. (1995) Structure and pharmacology of γ-aminobutyric acid A receptor subtypes. *Pharmacol. Rev. 47*, 181−234.
(32) Carlson, B. X., Hales, T. G., and Olsen, R. W. (1997) $GABA_A$ Receptors and Anesthesia. In *Anesthesia: Biologic Foundations* (Yaksh, T. L., et al., Ed.) pp 259−275, Lippincott-Raven Publishers, Philadelphia.
(33) Jenkins, A., Greenblatt, E. P., Faulkner, H. J., Bertaccini, E., Light, A., Lin, A., Andreasen, A., Viner, A., Trudell, J. R., and Harrison, N. L. (2001) Evidence for a common binding cavity for three general anesthetics within the $GABA_A$ receptor. *J. Neurosci. 21*, U7−U10.
(34) Chiara, D. C., Dangott, L. J., Eckenhoff, R. G., and Cohen, J. B. (2003) Identification of nicotinic acetylcholine receptor amino acids photolabeled by the volatile anesthetic halothane. *Biochemistry 42*, 13457−13467.
(35) Garcia, G., Chiara, D. C., Nirthanan, S., Hamouda, A. K., Stewart, D. S., and Cohen, J. B. (2007) [^{3}H]Benzophenone photolabeling identifies state-dependent changesin nicotinic acetylcholine receptor structure. *Biochemistry 46*, 10296−10307.
(36) Chiara, D. C., Hong, F. H., Arevalo, E., Husain, S. S., Miller, K. W., Forman, S. A., and Cohen, J. B. (2009) Time-resolved photolabeling of the nicotinic acetylcholine receptor by [^{3}H]-azietomidate, an open-state inhibitor. *Mol. Pharmacol. 75*, 1084−1095.
(37) Yamodo, I. H., Chiara, D. C., Cohen, J. B., and Miller, K. W. (2010) Conformational changes in the nicotinic acetylcholine receptor during gating and desensitization. *Biochemistry 49*, 156−165.
(38) Hamouda, A. K., Stewart, D. S., Husain, S. S., and Cohen, J. B. (2011) Multiple transmembrane binding sites for p-trifluoromethyldiazirinyl-etomidate, a photoreactive *Torpedo* nicotinic acetylcholine receptor allosteric inhibitor. *J. Biol. Chem. 286*, 20466−20477.
(39) Bali, M., and Akabas, M. H. (2004) Defining the propofol binding site location on the $GABA_A$ receptor. *Mol. Pharmacol. 65*, 68−76.
(40) Li, G. D., Chiara, D. C., Cohen, J. B., and Olsen, R. W. (2010) Numerous classes of general anesthetics inhibit etomidate binding to γ-aminobutyric acid type A ($GABA_A$) receptors. *J. Biol. Chem. 285*, 8615−8620.
(41) Li, G.-D., Chiara, D. C., Cohen, J. B., and Olsen, R. W. (2009) Neurosteroids allosterically modulate binding of the anesthetic etomidate to γ-aminobutyric acid type A receptors. *J. Biol. Chem. 284*, 11771−11775.
(42) Bertaccini, E. J., Wallner, B., Trudell, J. R., and Lindahl, E. (2010) Modeling anesthetic binding sites within the glycine α1 receptor based on prokaryotic ion channel templates: The problem with TM4. *J. Chem. Inf. Model. 50*, 2248−2255.
(43) Hall, M. A., Xi, J., Lor, C., Dai, S., Pearce, R., Dailey, W. P., and Eckenhoff, R. G. (2010) *m*-Azipropofol (AziPm) a photoactive analogue of the intravenous general anesthetic propofol. *J. Med. Chem. 53*, 5667−5675.
(44) Darbandi-Tonkabon, R., Hastings, W. R., Zeng, C.-M., Akk, G., Manion, B. D., Bracamontes, J. R., Steinbach, J. H., Mennerick, S., Covey, D. F., and Evers, A. S. (2003) Photoaffinity labeling with a neuroactive steroid analogue. *J. Biol. Chem. 278*, 13196−13206.
(45) Eckenhoff, R. G., Xi, J., Shimaoka, M., Bhattacharji, A., Covarrubias, M., and Dailey, W. P. (2010) Azi-isoflurane, a photolabel analog of the commonly used inhaled general anesthetic isoflurane. *ACS Chem. Neurosci. 1*, 139−145.
(46) Chiara, D. C., Hamouda, A. K., Ziebell, M. R., Mejia, L. A., Garcia, G., and Cohen, J. B. (2009) [^{3}H]Chlorpromazine photolabeling of the *Torpedo* nicotinic acetylcholine receptor identifies two state-dependent binding sites in the ion channel. *Biochemistry 48*, 10066−10077.